Supporting information

A cucurbituril-pillararene ring-on-ring complex

https://doi.org/10.1039/D1CC01777B

Dejun Zhang,[a] Hao Tang,*[a] Guozhen Zhang,*[b] Lingyun Wang,[a] Derong Cao*[a]

[a]State Key Laboratory of Luminescent Materials and Devices, School of Chemistry and Chemical Engineering, South China University of Technology, Guangzhou 510640, China.

haotang@scut.edu.cn, drcao@scut.edu.cn

[b]Hefei National Laboratory for Physical Sciences at the Microscale, iChEM, School of Chemistry and Materials Science, University of Science and Technology of China, Hefei, Anhui 230026, China.

guozhen@ustc.edu.cn

Contents

Experimental details.

Materials and Equipment. TPT[5] ($C_{85}H_{150}Br_{10}N_{10}O_{10}$), CB[10] ($C_{60}H_{60}N_{40}O_{20}$), and CB[8] ($C_{48}H_{48}N_{32}O_{16}$) samples were prepared as previously reported[1, 2]. G1 ($C_5H_{11}NaO_3S$, Energy Chemical, 99%), G2 ($C_4H_8Na_2O_6S_2$, Energy Chemical, 99%) and G3 ($C_{25}H_{16}$, Energy Chemical, 98 %) were used without further purification.

Solution preparation. The deionized water obtained from an ELGA PureLab Ultra Genetic system (≥ 18.2 MΩ cm^{-1}) was used as solvent to prepare all aqueous solutions except that stock solution of G3 was prepared by dissolving the solid into methanol. The appropriate amount of the stock solutions was injected into the deionized water and obtained the lower concentration of samples. The samples used for absorption and steady-state fluorescence experiments were hold in the 10 mm × 10 mm quartz cells. Those samples were thermostated at 20.0 ± 0.2 °C for at least 10 min before the experiments.

Equipment and methods. A Bruker DRX-500 spectrometer was used to collect the ^{1}H NMR spectra. The UV-Vis absorption spectra were measured by a Shimadzu UV-2600. The steady-state fluorescence spectra were collected on a Hitachi F-7000 with 2.5 nm of the bandwidths for both of excitation and emission channels. The excitation wavelength was set at 289 nm to obtain the emission spectra.

The computational study. All first-principle calculations were performed in water using semi-empirical tight binding method as implemented in xtb 6.3.3 by Grimme and co-workers.[3] The solvent effect of water was treated implicitly via a PCM solvation model.

The proton NMR spectra for CB[10]/TPT[5] systems.

The NMR spectra of CB[10]/TPT[5] systems were determined 5 min after adding TPT[5] in the D_2O containing solid CB[10]. When the amount of TPT[5] was half of CB[10], CB[10] was fully dissolved and the signals for the protons in the side arms of TPT[5] ($H^{1a–1c}$) shifted slightly upfield, indicating the

formation of CB[10]•TPT[5]•CB[10] . The signals for the protons in the side arms of TPT[5] ($H^{1a–1c}$) shifted slightly upfield (0.05–0.17 ppm), whereas those for the protons close to the pillar[5]arene cavity ($H^{1d–1e}$) barely shifted (< 0.03 ppm), suggesting that the former protons were close to the binding sites but the latter ones are not. When the amount of TPT[5] was equivalent and double of CB[10], the protons in the side arms of TPT[5] ($H^{1a–1c}$) shifted slightly downfield. The protons of methyl groups for TPT[5] were 3.0889, 3.1341 and 3.1904 ppm when the ratio of TPT[5]/CB[10] were 1:2, 1:1 and 2:1, respectively, indicating that the species of TPT[5] free in the solution and TPT[5] bound to the CB[10] coexist in the systems and eliminating the formation of TPT[5]•CB[10]•TPT[5]. The protons in the side arms of TPT[5] ($H^{1a–1c}$) didn't shift upfield if the formation of TPT[5]•CB[10]•TPT[5] was observed. Moreover, the fluorescence titration experiments for the binding between G1 and TPT[5]•CB[10] indicated that CB[10]•TPT[5]•CB[10] should not be major component when the ratio of TPT[5]/CB[10] were higher than 1:1 (see discussion in the below). Meantime, the binding of G1 to CB[10]•TPT[5]•CB[10] should lead to the precipitation of CB[10], which was not observed in the CB[10]/TPT[5]/G1 system. Our results indicated that TPT[5] could bind the second CB[10] to result in a 1:2 stoichiometry if the ratio of TPT[5]/CB[10] was lower 1:1. When the ratio of TPT[5]/CB[10] was higher 1:1, the major species was TPT[5]•CB[10], and CB[10]•TPT[5]•CB[10] should not be the major component.

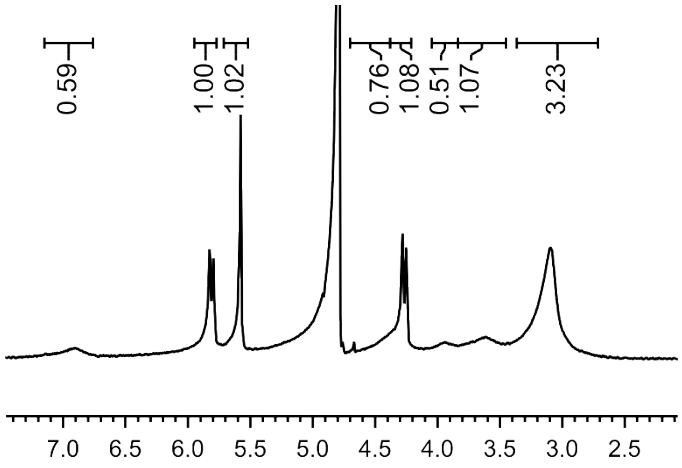

Figure S1. ^{1}H NMR spectra (D_2O, 298 K, 500 MHz) of CB[10] with 0.5 eq TPT[5] determined 5 min after mixing. [CB[10]]= 2.0 mM.

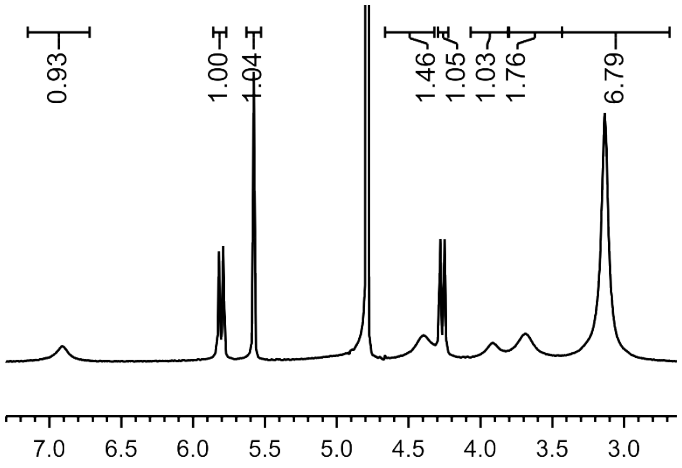

Figure S2. ^{1}H NMR spectra (D_2O, 298 K, 500 MHz) of CB[10] with 1 eq TPT[5] determined 5 min after mixing. [CB[10]]= 2.0 mM.

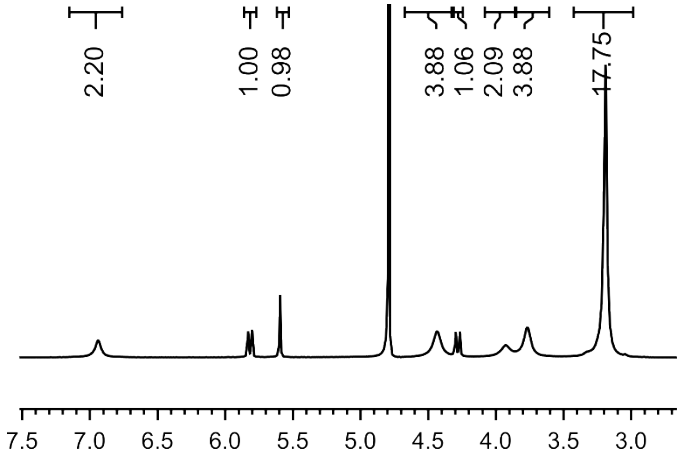

Figure S3. ^{1}H NMR spectra (D_2O, 298 K, 500 MHz) of 2.0 mM CB[10] with 2 eq TPT[5] determined 5 min after mixing. [CB[10]]= 2.0 mM.

The proton NMR spectra for CB[8]/TPT[5] systems.

The ^{1}H NMR spectra for the CB[8]/TPT[5] systems were determined 20 min and 2 days after mixing the CB[8] solid (~1 equiv) and the TPT[5] solution. All protons in CB[8] appeared over 20 min and then increased to a small extent (black arrows) over 2 days. Meantime, the proton in TPT[5] (H^{1a}) shifted slightly upfield, while other protons did not obviously shift, indicating that only the trimethylammonium groups in TPT[5] were close to the portal of CB[8] to form an exclusion complex (TPT[5]•CB[8]). According to the peak integration ratio of CB[8] to TPT[5], the binding affinity of TPT[5] to CB[8] was significantly lower than that to CB[10].

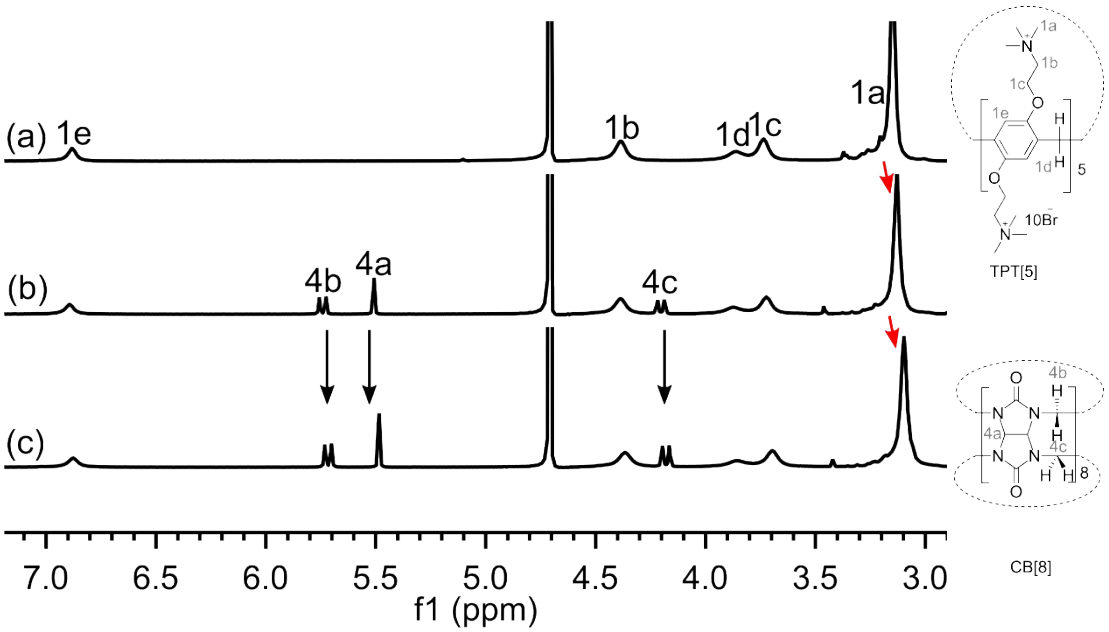

Figure S4. ^{1}H NMR spectra (D_2O, 298 K, 500 MHz) of (a) TPT[5], (b) CB[8]/TPT[5] mixed for 20 min and (c) CB[8]/TPT[5] mixed for 2 days. [TPT[5]] = 2 mM.

The proton NMR spectra for TPT[5]•CB[10]/G1 systems.

The CB[10] solid (~1 equiv) was dissolved into the solution of TPT[5] to form TPT[5]•CB[10] complex followed by the addition of the G1 solid (~10 equiv). This mixing solution was investigated by ^{1}H NMR spectroscopy after 5 min and 2 days. The NMR spectrum determined after 5 min was similar with that

determined after 2 days (Figure 3).

The proton NMR spectra for G1@TPT[5]/CB[10] systems.

The D_2O solutions of G1 (~10 equiv) and TPT[5] were mixed first to form G1@TPT[5] complex followed by addition of the CB[10] solid (~1 equiv). After 5 min and 2 days, this mixing solution was investigated by ^1H NMR spectroscopy, respectively. All CB[10] solid disappeared and the protons in CB[10] (H^{3a-3c}) were observed in the Figure S5b, indicated the formation of ternary complex (G1@TPT[5]•CB[10]). In addition, all protons in G1 ($H^{1\alpha-1\varepsilon}$) shifted upfield to a small extent, and the proton in TPT[5] (H^{1a}) shifted slightly upfield. The NMR spectrum determined after 2 days was similar to that determined after 5 min.

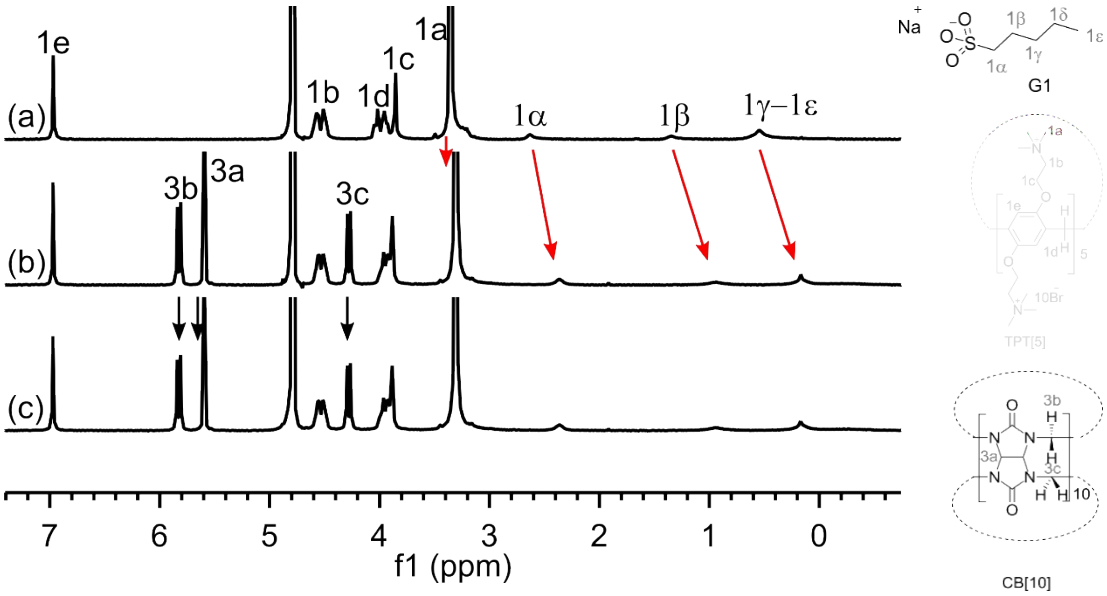

Figure S5. ^1H NMR spectra (D_2O, 298 K, 500 MHz) of (a) G1@TPT[5], (b) G1@TPT[5]/CB[10] mixed for 5 min, (c) G1@TPT[5]/CB[10] mixed for 2 days. [TPT[5]] = 2 mM. [G1] = 20 mM.

Absorption and fluorescence spectra for the TPT[5]•CB[10]/G1 systems.

The absorption peak at 289 nm and the fluorescence peak at 321 nm for TPT[5] decreased, but not shifted when it bound to CB[10]. For the binding of G1 to TPT[5]•CB[10], the peaks were enhanced in both spectra. A red shift of 2 nm and a blue shift of 2 nm were observed for peaks in the absorption and

the fluorescence spectra, respectively.

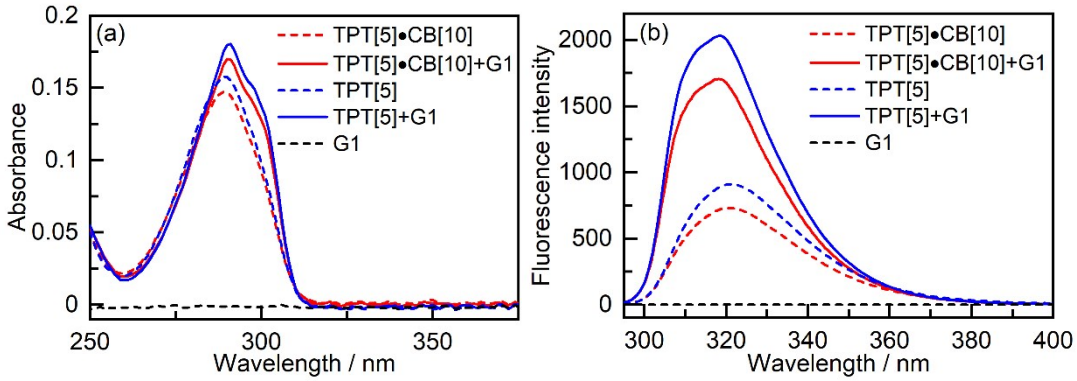

Figure S6. Absorption (a) and fluorescence spectra (b) for TPT[5]•CB[10], TPT[5], G1, TPT[5]/G1 and TPT[5]•CB[10]/G1 aqueous solutions. [TPT[5]•CB[10]] = 10 μM. [TPT[5]] = 10 μM. [G1] = 30 μM.

Binding isotherm for the formation of the TPT[5]•CB[10]/G1 systems.

The fluorescence titration experiments were performed where the concentration of one species was fixed as the constant and the other one gradually varied. The dependence of the fluorescence intensity (I_{int}) on the G1 concentration was fit numerically by using Scientist 3 from Micromath.

The binding constant (K) for the formation of G1@TPT[5]•CB[10] complex (Scheme S1) were determined by using an example as follows. The total concentration of the G1 ($[G1]_T$) gradually increased, while that of host ($[TPT[5]•CB[10]]_T$) was fixed as a constant. The fluorescence intensity of TPT[5]•CB[10] (I_{int}) determined for each sample was related to the sum of the two terms (eq. S2) where each term was the product of the fluorescence quantum yield (Φ) of each species and its concentration in the system. The relationship between [TPT[5]•CB[10]] and [G1@TPT[5]•CB[10]] was defined by the binding constant (K, Scheme S1) and the mass balance equations (eq. S4 and S5).

$$\text{TPT[5]•CB[10]} + \text{G1} \overset{K}{\rightleftharpoons} \text{G1@TPT[5]•CB[10]} \qquad \text{(S1)}$$

Scheme S1. Overall equilibrium for the formation of the G1@TPT[5]•CB[10] complex.

$$I_{int} = \Phi_1 \times [TPT[5]•CB[10]]_{eq} + \Phi_2 \times [G1@TPT[5]•CB[10]]_{eq} \qquad \text{(S2)}$$

The model used in Scientist 3 was listed as follows: The independent variable was the total

concentration of G1 ($[G1]_T$). The dependent variables were I_{int} and the concentrations of each species at equilibrium, which included free TPT[5]•CB[10] ($[TPT[5]•CB[10]]_{eq}$), free G1 ($[G1]_{eq}$), and 1:1 G1@TPT[5]•CB[10] exclusion complex ($[G1@TPT[5]•CB[10]]_{eq}$). The parameters were the binding constant (K) and the fluorescence quantum yields for each TPT[5]•CB[10] species, including Φ_1 for free TPT[5]•CB[10] and Φ_2 for G1@TPT[5]•CB[10]. The fluorescence intensity of TPT[5]•CB[10] in the absence of the G1 was defined as I_0.

The equations for this model were listed as follows:

$$[G1@TPT[5]•CB[10]]_{eq} = K \times [TPT[5]•CB[10]]_{eq} \times [G1]_{eq} \quad \text{(S3)}$$

$$[TPT[5]•CB[10]]_{eq} = [TPT[5]•CB[10]]_T - [G1@TPT[5]•CB[10]]_{eq} \quad \text{(S4)}$$

$$[G1]_{eq} = [G1]_T - [G1@TPT[5]•CB[10]]_{eq} \quad \text{(S5)}$$

$$I_0 = \Phi_1 \times [TPT[5]•CB[10]]_T \quad \text{(S6)}$$

$$\frac{I_{int} - I_0}{I_0} = \frac{(\Phi_2 - \Phi_1) \times [G1@TPT[5]•CB[10]]_{eq}}{\Phi_1 \times [TPT[5]•CB[10]]_T} \quad \text{(S7)}$$

Ranges for the dependent variables were listed as follows:

$$0 < [G1]_{eq} < [G1]_T \quad \text{(S8)}$$

$$0 < [TPT[5]•CB[10]]_{eq} < [TPT[5]•CB[10]]_T \quad \text{(S9)}$$

$$0 < [G1@TPT[5]•CB[10]]_{eq} < [TPT[5]•CB[10]]_T \quad \text{(S10)}$$

The binding constant for G1@complex was (3.7 ± 0.1) × 10^6 M^{-1}, which is very close to that for G1@TPT[5] determined before ((3.8 ± 0.4) × 10^6 M^{-1}), indicating the TPT[5], whether it was bound to CB[10] or not, has almost the same binding affinity to G1. This result shows that CB[10] did not compete with G1 to TPT[5].

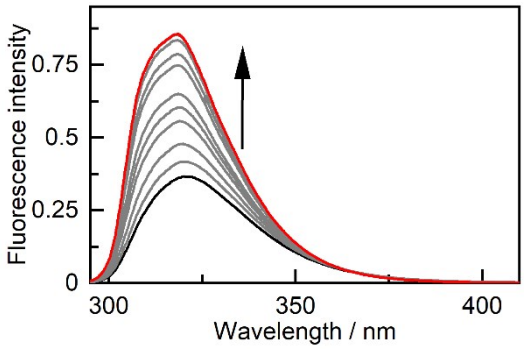

Figure S7. Dependence of the fluorescence emission spectra of TPT[5]•CB[10] on the concentration of G1. λ_{ex} = 291 nm. [TPT[5]•CB[10]] = 10 μM. From bottom to top, [G1] = 0, 1, 2, 4, 5, 6, 8, 12, 20, 30 and 50 μM.

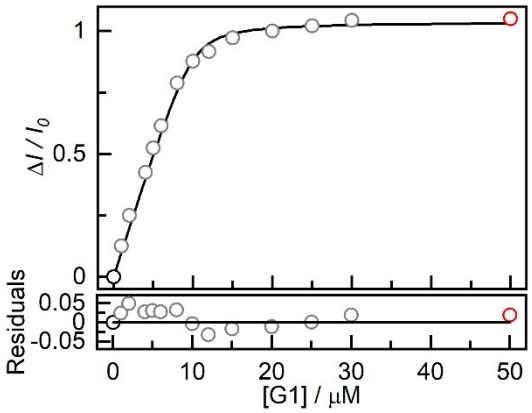

Figure S8. Binding isotherm for the complexation of TPT[5]•CB[10] with G1. The data was fitted by using a 1:1 binding model. The bottom panel was shown in the residuals between the fit and the experimental data. [TPT[5]•CB[10]] = 10 μM. λ_{ex} = 291 nm.

The computational result for G1@TPT[5]•CB[10]/ systems.

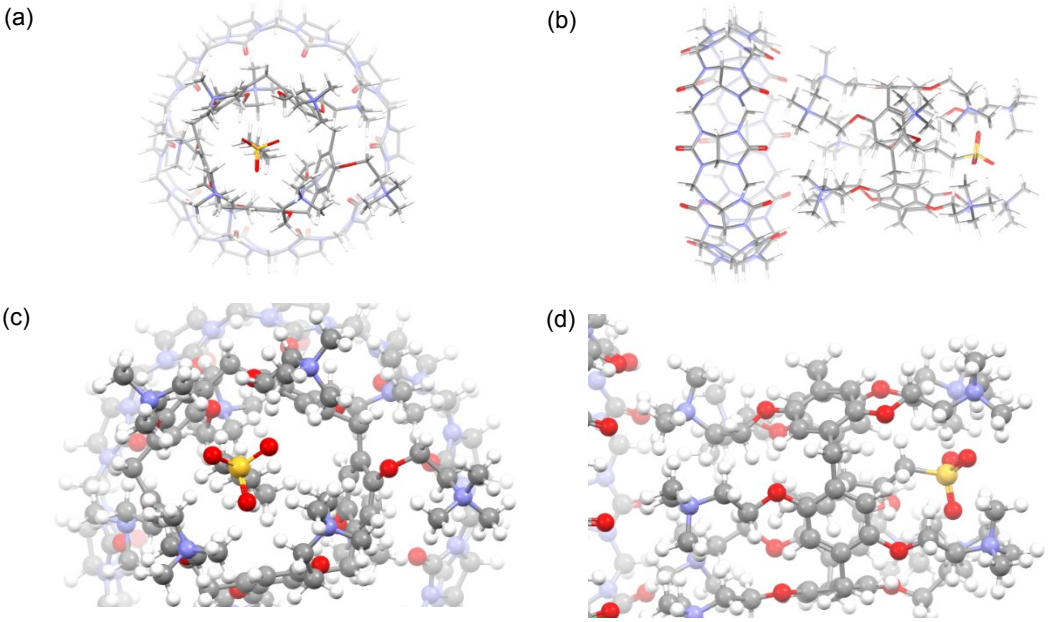

Figure S9. The computational result of G1@TPT[5]•CB[10] complexes. Panels a and b are top and side view of the structure, respectively. Panels c and d are the zoom-in view showing the binding sites.

The proton NMR experiment to check the purity of CB[10].

The sample of purified solid CB[10] was added in TPT[5] solution to form the TPT[5]•CB[10] complex and were then investigated by ^{1}H NMR spectroscopy. Only proton signals of CB[10] were observed, while the proton signals of other CB[5-8] were not, indicating that the pure CB[10] was successfully isolated from crude CB[5-8, 10] (Figure S10). Our route (Route 1 in Figure S11) required three steps and five days. By contrast, the conventional isolation route (Route 2 in Figure S11) took about two weeks and six steps, including dissolving the sample in 6 M HCl, precipitating the sample by 3,5-dimethyladamantanamine (G4), and washing the sample by 6 M HCl, DMSO, CH_3OH and H_2O sequentially. 17 mg of pure CB[10] was obtained from 1 g of crude CB[n] using our method, while 29 mg of pure CB[10] was obtained from 1 g of crude CB[n] using the conventional method[2].

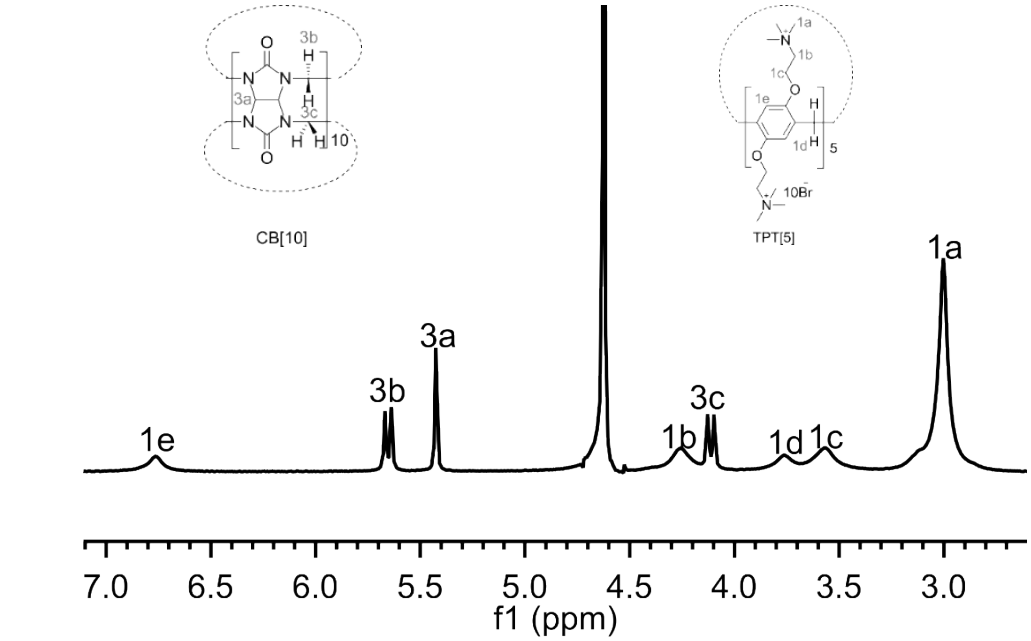

Figure S10. ^{1}H NMR spectra (D_2O, 298 K, 500 MHz) for TPT[5]•CB[10].

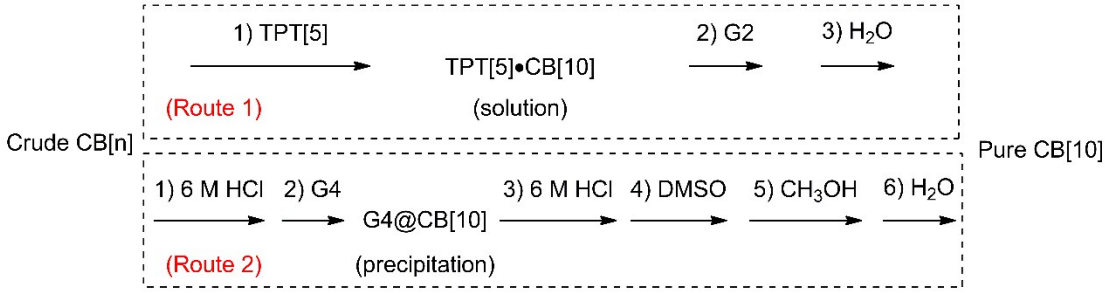

Figure S11. Separation routes of pure CB[10] from crude CB[n] mixture.

Absorption and fluorescence spectra for the TPT[5]•CB[10]/G3 systems.

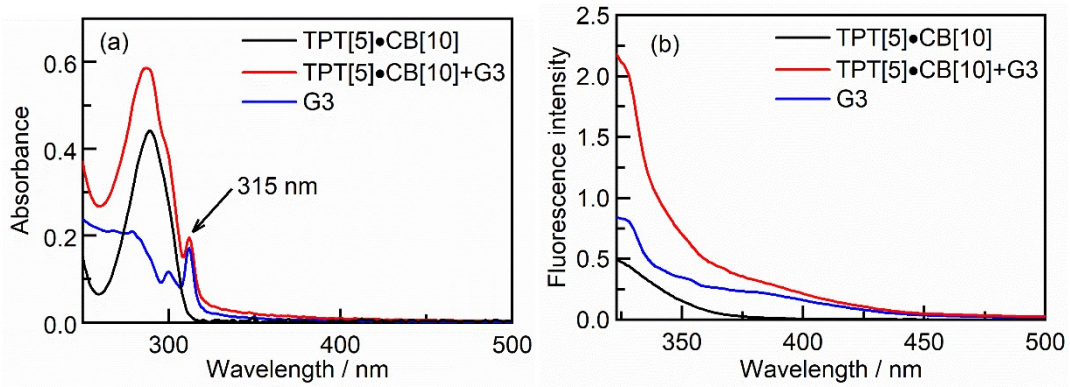

Figure S12. Absorption (a) and fluorescence spectra (b) for the aqueous solutions of TPT[5]•CB[10], G3 and TPT[5]•CB[10]/G3 systems. [TPT[5]•CB[10]] = 30 μM. [G3] = 10 μM. λ_{ex} = 315 nm.

Binding isotherm for the formation of the G3@CB[10]•TPT[5] complex.

The absorption peak at 315 nm for G3 was selected as the excitation wavelength in the fluorescence experiments. The control experiments were performed by preparing solutions that contained all chemicals with the exception of G3. Fluorescence spectrum for each G3@CB[10]•TPT[5] sample was corrected by subtracting the fluorescence spectrum of corresponding control sample under the same experimental condition. The fluorescence peak over 325 nm for G3 gradually increased with the addition of TPT[5]•CB[10] (see the inset in figure S13). The fitting procedure and the mode were similar to the determination for the binding constant for the formation of G1@TPT[5]•CB[10] complex (see above) expect that the terms for G1 and TPT[5]•CB[10] were replaced by the terms for TPT[5]•CB[10] and G3, respectively.

The binding isotherms obtained from two independent experiments were fitted well with a 1:1 host-guest binding model, which gave a value of (3.3 ± 0.7) × 10^5 M^{-1} as the binding constant (*K*) for the complexation of G3 by TPT[5]•CB[10].

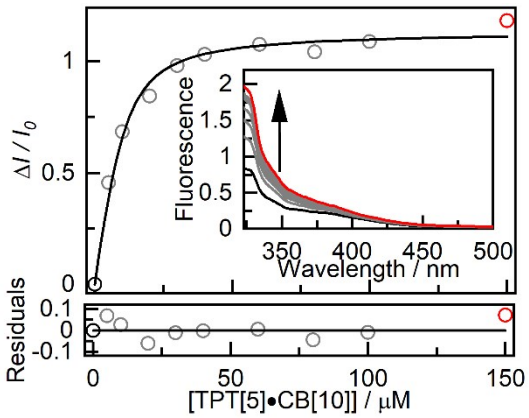

Figure S13. Binding isotherm for the complexation of TPT[5]•CB[10] with G3. The data was fitted with a 1:1 binding model. The inset shows the dependence of the corrected fluorescence emission of G3 on the concentration of TPT[5]•CB[10]. The bottom panel shows the residuals between the fit and the experimental data. λ_{ex} = 315 nm. [G3] = 10 μM.

1. Y. J. Ma, X. F. Ji, F. Xiang, X. D. Chi, C. Y. Han, J. M. He, Z. Abliz, W. X. Chen and F. H. Huang, *Chem. Commun.*, 2011, **47**, 12340-12342.
2. X. Yang, Z. Zhao, X. Zhang and S. Liu, *Sci. China Chem.*, 2018, **61**, 787-791.
3. C. Bannwarth, E. Caldeweyher, S. Ehlert, A. Hansen, P. Pracht, J. Seibert, S. Spicher and S. Grimme, *WIREs Computational Molecular Science*, 2020, **11**.